Supporting Information

Practical high strain with superior temperature stability in lead-free piezoceramics through domain engineering

Chunlin Zhao[1], Bo Wu[1, 3], Ke Wang[2,*], Jing-Feng Li[2], Dingquan Xiao,[1] Jianguo Zhu,[1] and Jiagang Wu[1,*]

[1]*Department of Materials Science, Sichuan University, Chengdu 610064, P. R. China*

[2]*State Key Laboratory of New Ceramics and Fine Processing, School of Materials Science and Engineering, Tsinghua University, Beijing 100084, P. R. China*

[3]*Sichuan Province Key Laboratory of Information Materials and Devices Application Chengdu University of Information Technology Chengdu People's Republic of China*

*Corresponding author. Email: msewujg@scu.edu.cn and wujiagang0208@163.com (J. W.); wang-ke@tsinghua.edu.cn (K. W.)

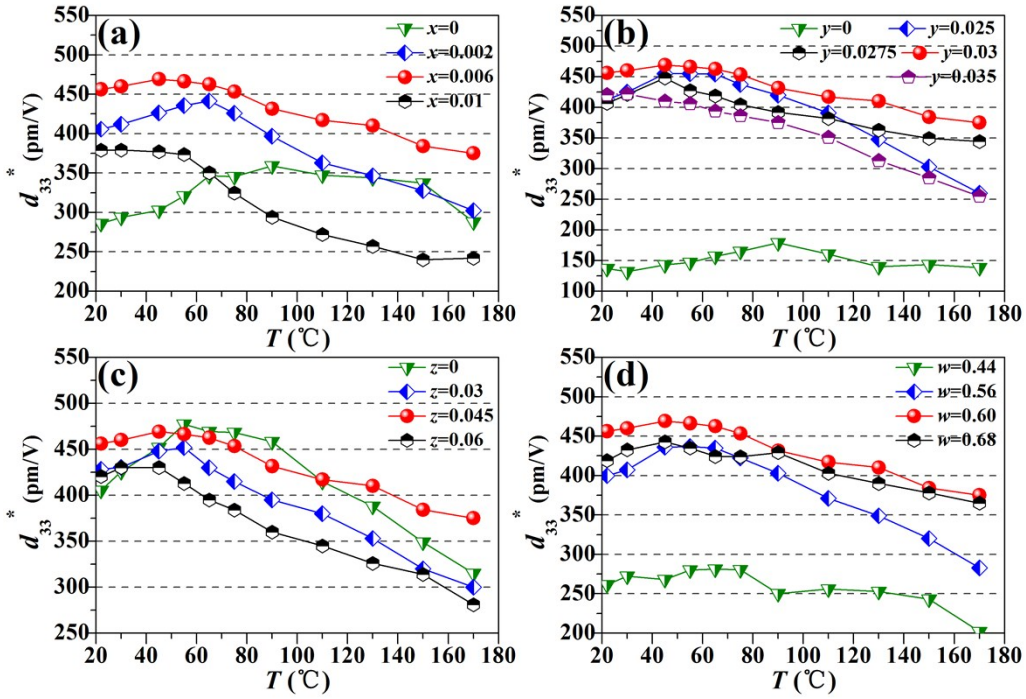

Fig. S1 Temperature-dependent normalized unipolar piezoelectric strain (d_{33}^*) for KN_wNS_z-xBF-yBNZ ceramics with (a) $0 \le x \le 0.01$ (y=0.03, z=0.045, w=0.6), (b) $0.025 \le y \le 0.035$ (x=0.006, z=0.045, w=0.6), (c) $0 \le z \le 0.06$ (x=0.006, y=0.03, w=0.6), and (d) $0.44 \le w \le 0.68$ (x=0.006, y=0.03, z=0.045).

Figure S1 displays the temperature/composition-dependent unipolar strain (d_{33}^*) of KN_wNS_z-xBF-yBNZ ceramics from room temperature to 170 °C as a function of x, y, z, and w, measured at 4 kV/mm. Distinct temperature stability and incipient-values on d_{33}^* are observed for different compositions. The high d_{33}^* of ~400-465 pm/V can be achieved due to the formation of phase boundaries. One can see that high d_{33}^* values always locate at the temperature region of phase boundaries, and slightly fluctuated d_{33}^* with maintaining than 80%-90% compared to room-temperature values is attained in this region.

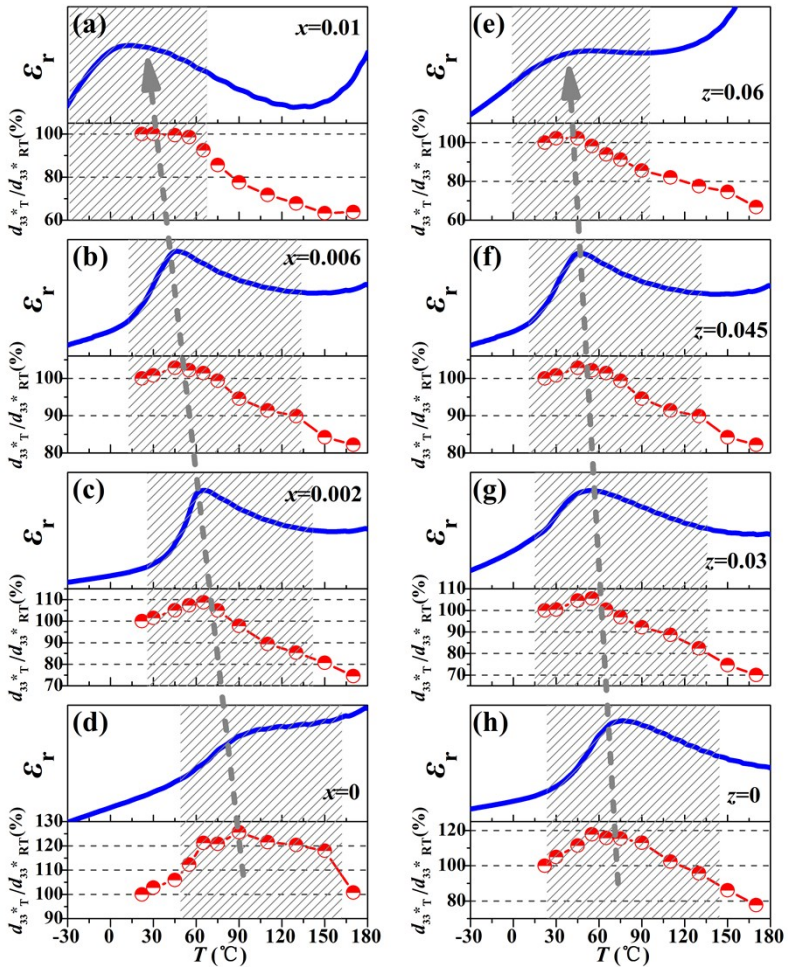

Fig. S2 Comparison of temperature-dependent dielectric constant (ε_r-T) curves [1] and normalized d_{33}^* (measured at 4 kV/mm) against their room-temperature values as a function of (a)-(d) x and (e)-(h) z for KN_wNS_z-xBF-yBNZ ceramics.

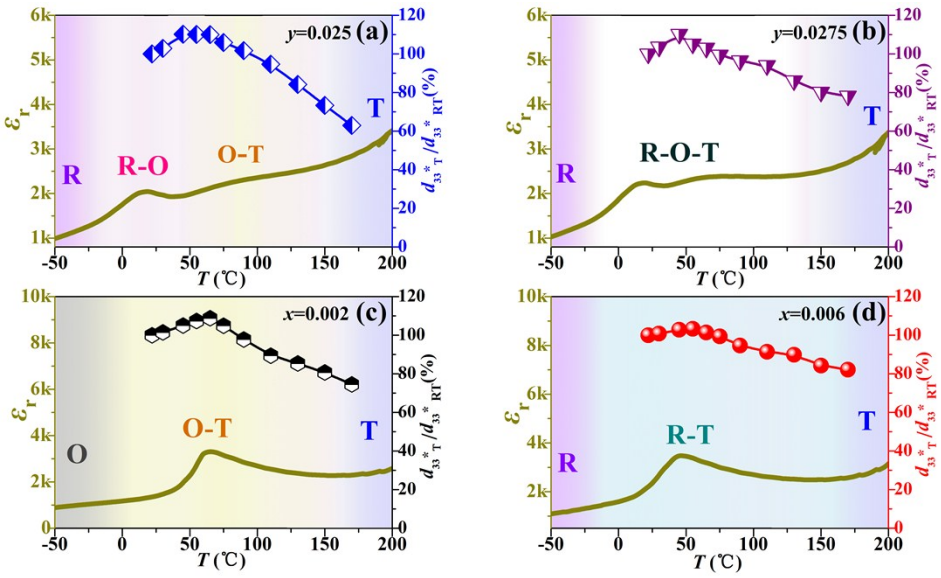

Fig. S3 Temperature dependence of $d_{33}^*$and dielectric constant ε_r [1] for the ceramics with (a) R-O, (b) R-O-T, (c) O-T, and (d) R-T phase boundary at room temperature.

Figure S2 displays the ε_r-T curves (cited from the previous work)[1] and normalized d_{33}^* against their room-temperature values as a function of x and z for KN_wNS_z-xBF-yBNZ ceramics. It can be seen that the high d_{33}^* value always appear in the temperature region of phase transition (phase boundary). When the phase boundary zone shifts to low temperature with increasing x or z, the temperature range of optimized d_{33}^* also shifts to corresponded temperature scope, and the maximum d_{33}^* usually appear in the temperature point of dielectric peak for ε_r-T curves. As a result, the strain property can be improved at phase boundary, and the strain fluctuation originates from the improvement effect on piezoelectricity induced by phase boundary. In addition, the strain fluctuation displays different behavior at different phase boundary, and the ceramic with R-T phase boundary present best temperature stability at phase boundary region, as shown in Figure S3.

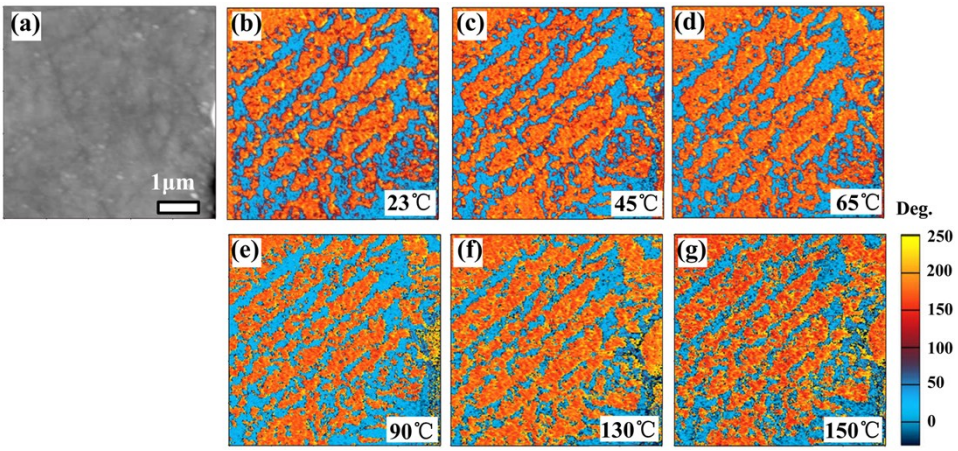

Fig. S4 Vertical piezoresponse force microscopy (V-PFM) images of phase at different temperature for KN_wNS_z-xBF-yBNZ (x=0.006) ceramics.

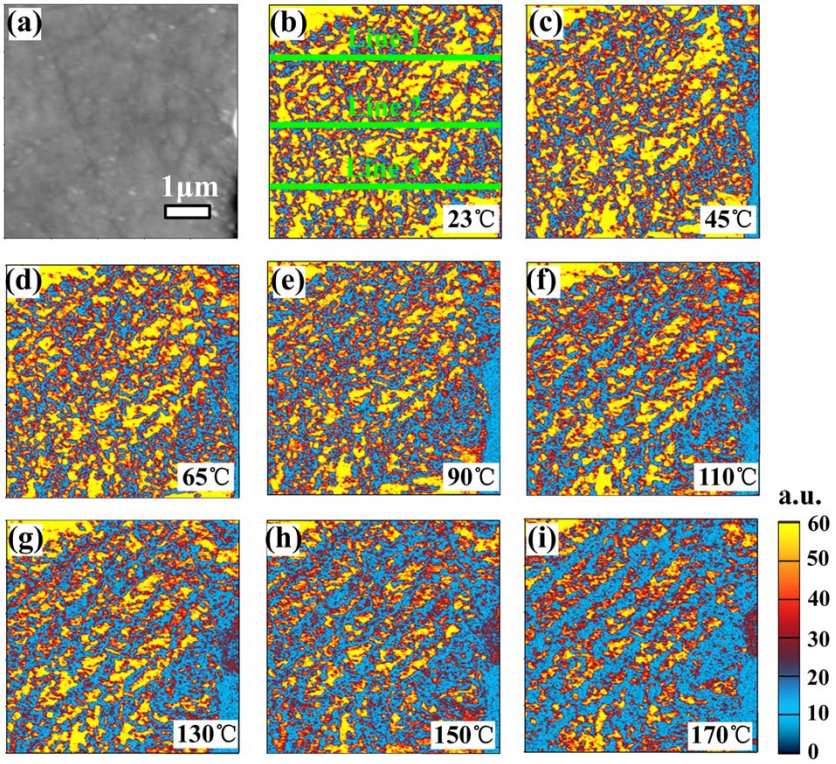

Fig. S5 Vertical piezoresponse force microscopy (V-PFM) images of amplitude at different temperature for KN_wNS_z-xBF-yBNZ (x=0.006) ceramics.

Figure S4 presents PFM phase evolution with temperature, and corresponding temperature dependence of amplitude image of PFM is presented in Figure S5. No

obvious changes were observed in the phase images from 23 to 170 °C, indicating the the configuration of virgin domains basically unchanges with increasing tempearutre. Nevertheless, the virgin domains resemble gradual decrease presented in their amplitude images when rise the temperature, as displayed in Fig. S5. This is actually the decreased number of active domains which still possess high piezoresponse at high temperature, and the average amplitude of all the virgin domains gradually decline under high temperature disturbance.

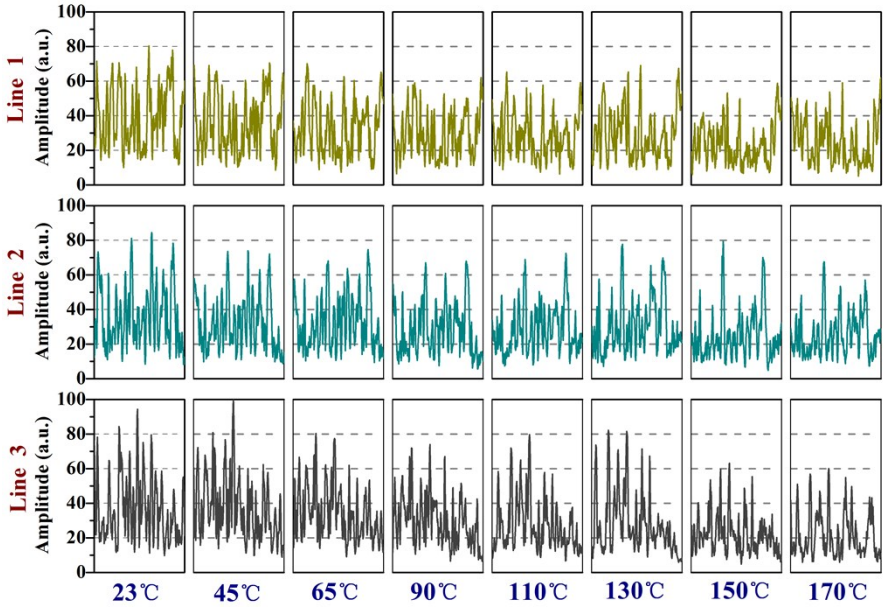

Fig. S6 Temperature-dependent piezoresponse amplitude profiles generated from the line scan (the position of "Line 1" to "Line 3" in Fig. S5) across the domains.

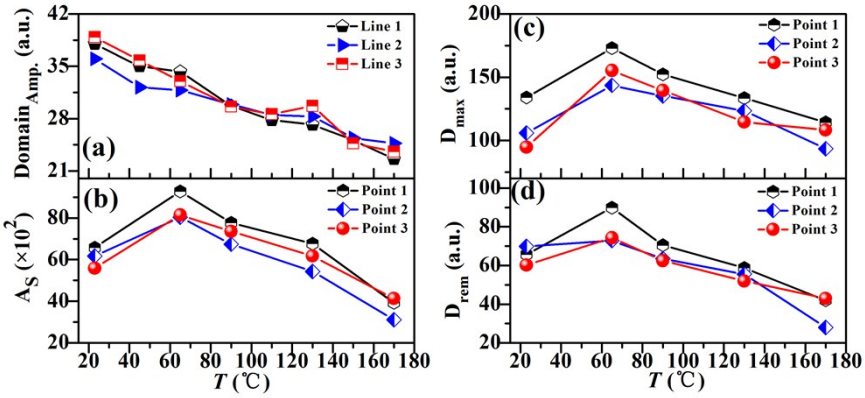

Fig. S7 (a) Temperature dependence of average piezoresponse amplitude evolution of

V-PFM images at different scan lines as the green lines in Fig. S4. (b)-(c) Temperature-dependent piezoresponse parameters with saturation piezoresponses D_{max}, remnant piezoresponses D_{rem}, and work of switching A_S for different local positions, measured by SS-PFM.

Figure S6 shows the temperature dependence of piezoresponse amplitude evolution at the position of "Line 1" to "Line 3". The results were carried out in the same position orientated by the surface morphology image [Fig. S5(a)] for each temperature point. Then all the amplitude values of each scan point in each scan line were summed. The change tendency of total value in each line can be regarded as the amplitude evolution of whole surface. And this result can be also proposed to the content evolution of high-piezoresponse domain. Finally, we obtain the average value in three different scan line as the high-piezoresponse domain content evolution under temperature disturbance. The results show in Figure S7(a). Figure S7(b)-(d) displays the temperature dependence of piezoresponse parameters (D_{max}, D_{rem}, and A_S) for local piezoresponse hysteresis loop measure different local positions. It can be seen that the piezoresponse parameters show close value for different measurement position, suggesting the measurement of piezoresponse hysteresis loop by SS-PFM can be exactly reflect the piezeresponse of local domain for the ceramics.

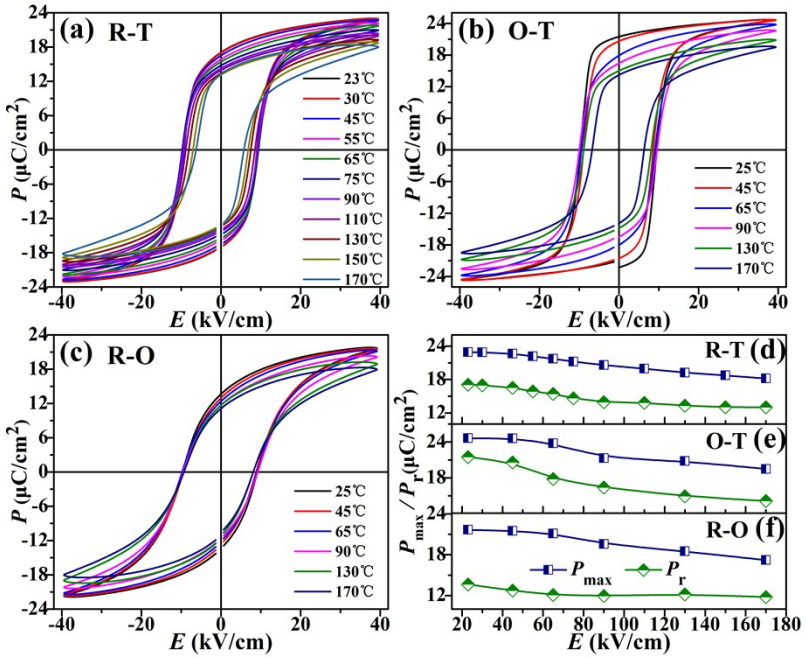

Fig. S8 Temperature-dependent ferroelectric hysteresis loops (*P*-*E*) for the ceramics with (a) R-T phase boundary, (b) O-T phase boundary, and (c) R-O phase boundary. Temperature-dependent related P_{max} and P_r values for the ceramics with (d) R-T phase boundary, (e) O-T phase boundary, and (f) R-O phase boundary.

Figure S8 presents temperature dependence of *P*-*E* loops for the ceramics with different phase boundary (R-T, O-T, or R-O), measured from 23 ^{o}C to 170 ^{o}C. It can be seen that the ferroelectric hysteresis loops for three phase boundary all gradually become slim when temperature increases. While, the maximum polarization P_{max} and remnant polarization P_r show different change tendency for these three phase boundary, as shown in Fig. S8(d)-(f).

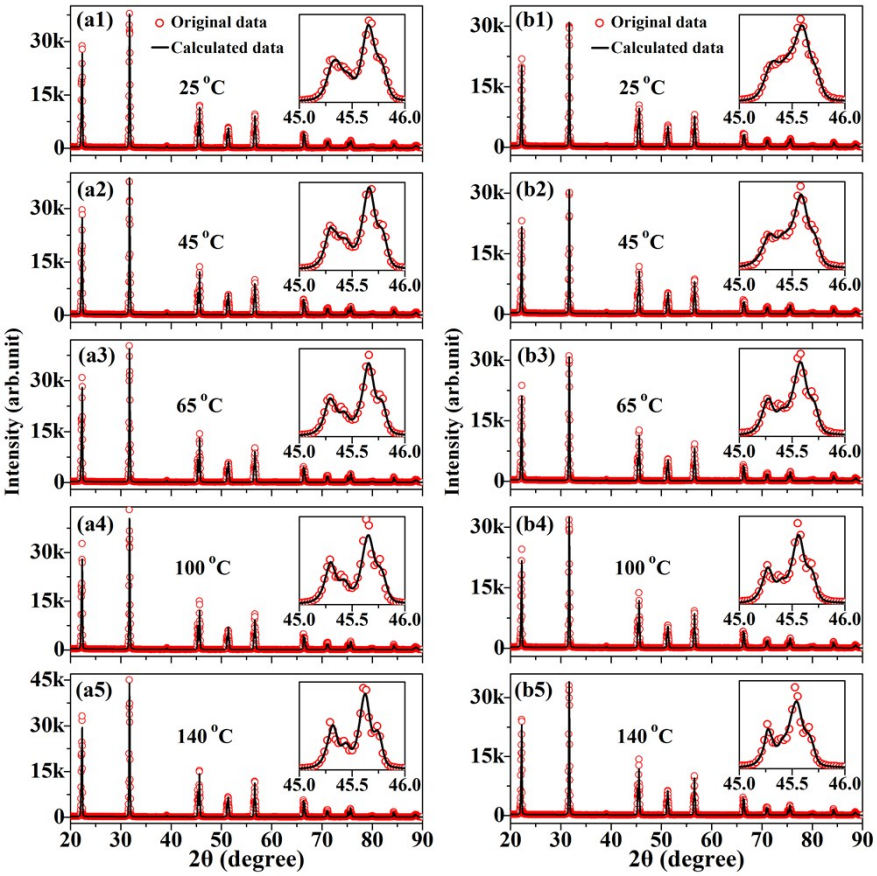

Fig. S9 Temperature-dependent XRD Rietveld refinement results of (a1)-(a5) y=0.0275 (R-O-T) and (b1)-(b5) x=0.006 (R-T).

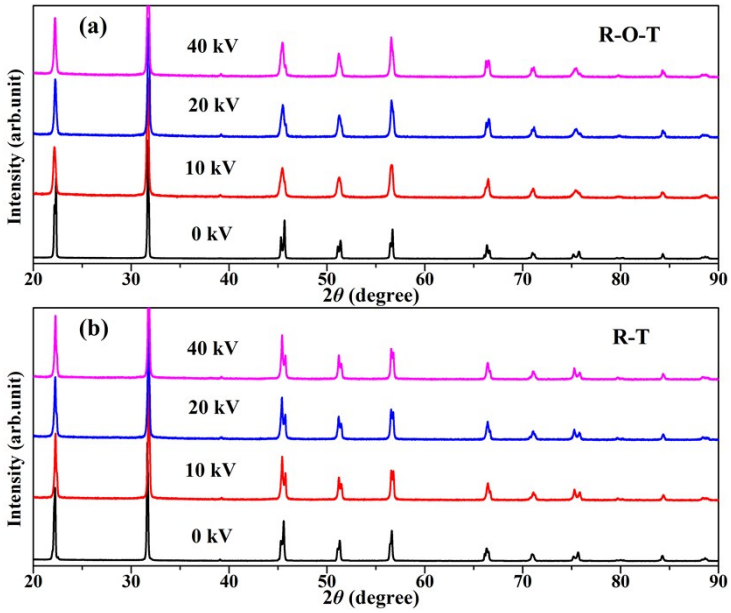

Fig. S10 Electric field-dependent XRD patterns of (a) R-O-T and (b) R-T phase

boundary measured at 0-40 kV/cm.

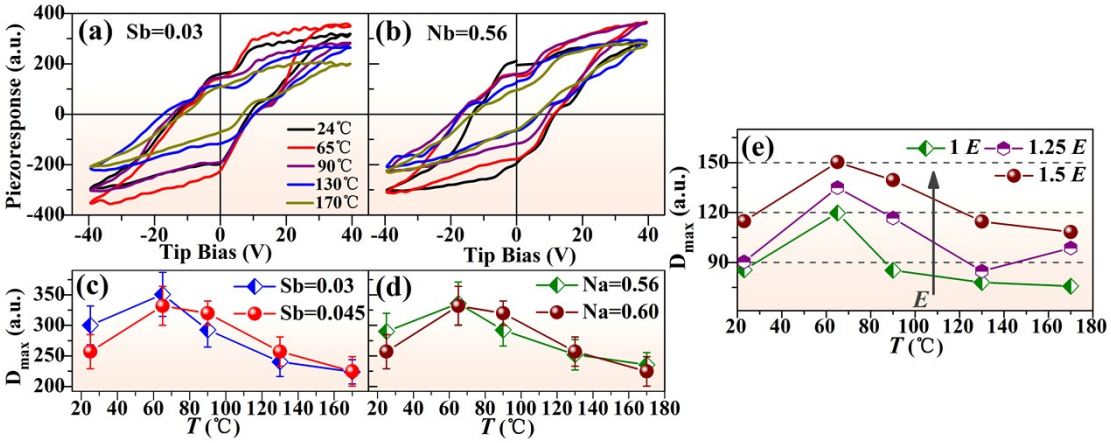

Fig. S11 (a)-(b) Temperature-dependent local piezoresponse hysteresis loops at R-T phase boundary with different Sb/Na contents. (c)-(d) Temperature-dependent piezoresponse parameters D_{max} with different Sb/Na contents. (e) Temperature-dependent piezoresponse parameters D_{max} at different tip bias voltages.

Figure S11(a)-(d) displays temperature dependence of local piezoresponse hysteresis loops of domain at R-T phase boundary with different Sb/Na contents. It can be seen that the samples with Sb/Na=0.045/0.6 present better temperature reliability of saturation piezoresponse D_{max} than the ones with low content (Sb/Na=0.03/0.56), finally resulting in a superior strain stability. Fig. S11(e) presents the bias voltage dependence of saturation piezoresponse D_{max} for ceramics with R-T phase boundary, measured at different temperature. We can see that the D_{max} improves when the bias voltage increases, while they gradually decrease with increasing temperature whatever the bias voltage is. However, it can be seen that the piezoresponse amplitude possesses a better temperature stability when the SS-PFM was carried out using a higher bias voltage.

References

1 B. Wu, H. Wu, J. Wu, D. Xiao, J. Zhu and S. J. Pennycook, *J. Am. Chem. Soc.*, 2016, **138**, 15459-15464.